




REGULAR ARTICLE

## Electrical and Mechanical Properties of Epoxy Composites Filled with Carbon and $\text{Co}_3\text{O}_4$ Nanoparticles

T.A. Len\* , V.V. Vovchenko, L.Yu. Matzui, O.V. Turkov, A.V. Zhuravkov

*Taras Shevchenko National University of Kyiv, Physical Faculty, 01601 Kyiv, Ukraine*

(Received 20 December 2023; revised manuscript received 17 February 2024; published online 28 February 2024)

The study of samples of multicomponent epoxy composites (CM) was carried out, the structure, morphology of fillers and their distribution in the epoxy matrix were studied, the features of the process of modifying the conductive cluster and changing the interphase polarization due to the integration of nanocarbon (graphite nanoplates GNP, carbon nanotubes CNT) and inorganic (Fe,  $\text{Co}_3\text{O}_4$ ) of superdisperse fillers, the influence of the composition, morphology and concentration of combined fillers on the electrodynamic characteristics of composites and the mechanisms of electrical transport in CM was determined. As shown by studies of the phase composition of magnetic powders by the X-ray diffraction method, cobalt oxide nanopowder consists of a pure  $\text{Co}_3\text{O}_4$  phase, and carbonyl iron – of pure  $\alpha$ -Fe. Experimental research of electrical resistance was carried out on direct current in the temperature range of 77-293 K. As studies have shown, the electrical conductivity of CM has a percolation character, that is, it increases sharply at a certain concentration (weight  $C_{cr}$  or volume  $\phi_c$ ) of the nanocarbon filler. The addition of inorganic fillers along with nanocarbon fillers leads to a change in the nature of the percolation curves. Changes in the electrical conductivity of three-phase CMs significantly depend on the size and morphology of nanocarbon particles.

The addition of nanocarbon filler GNP along with inorganic magnetic particles  $\text{Co}_3\text{O}_4$  or Fe led to a decrease in the percolation threshold and a higher electrical conductivity of CM at a GNP content higher than 3 wt. %. When adding  $\text{Co}_3\text{O}_4$  particles along with CNTs to the epoxy matrix, there are significant changes in the electrical conductivity at a CNT content of 1-5 wt. % was not observed.

The nature of the temperature dependence of the electrical resistance is different depending on the type and content of the two-component filler in the CM. For epoxy CMs with high electrical resistance, a significant decrease in electrical resistance is observed when heated from 77 to 293 K.

It was found, that the addition of 2-5 wt. % of graphite nanoparticles along with  $\text{Co}_3\text{O}_4$  nanoparticles decreases the effective Young modulus and the compression strength of three-phase composites compared with  $\text{Co}_3\text{O}_4$ /epoxy. 5CNT/ $\text{Co}_3\text{O}_4$ /epoxy CM showed the minimal value of Young modulus (520 MPa) and enhanced flexible properties compared with composites with GNP/ $\text{Co}_3\text{O}_4$  filler. The significant decrease in electric resistance (by 2 orders of magnitude) under uniaxial compression was found for 3GNP/ $\text{Co}_3\text{O}_4$ /epoxy CM with nanocarbon content close to the percolation threshold. The sufficiently lower reversible decrease of electrical resistance (not exceed 30 % relative to the initial value) was observed for 5 %GNP/ $\text{Co}_3\text{O}_4$ /epoxy composite.

**Keywords:** Cobalt oxide, Composite material, Carbonyl iron, Electrical conductivity, Mechanical properties.

DOI: [10.21272/jnep.16\(1\).01026](https://doi.org/10.21272/jnep.16(1).01026)

PACS number: 61.48.De

### 1. INTRODUCTION

Due to the rapid development of industrial technologies and the miniaturization of technological devices, the development of new electronic components for the electronic industry to work with higher power becomes important.

Therefore, to ensure the normal operation of devices, it is especially important to know the characteristics of materials for packaging electronic components, both individually and as part of composite materials. At the last time of receipt new materials with particular structure and properties by ease, green and cheap processing, has been an active topic, for both scientific standpoint and technological applications. By changing the nanomaterials dimensions or their blend, one can get new material that has different structures and innovative properties. The addition into polymer matrix

of nanofillers such as layered silicates, carbon nanotube, fullerene, metal nanoparticles exhibits favorable effect on improving the thermal stability, mechanical, and electrical properties of polymer composite materials simultaneously at low loading.

The mechanical and electrical properties of composites depend on the structural and morphological features of the CM components. The characteristics of the fillers, their distribution in the composite, and the conditions of preparation of multicomponent composites can change the thermal, electrical, and mechanical properties of the final material. The scientific interests of many researchers are aimed at obtaining and studying composite materials with a polymer matrix filled with nanocarbon fillers, such as graphene, carbon nanotubes, carbon nanofibers, which have a number of advantages due to its high surface area, chemical stability, unique electronic and outstanding mechanical properties.

\* Correspondence e-mail: [talen148@gmail.com](mailto:talen148@gmail.com)



Nanosized particles of transition metals and their oxides also have many advantages as fillers of polymer matrices due to their unique physical properties.

Among metal oxides, cobalt oxide ( $\text{Co}_3\text{O}_4$ ) is the most promising component at fabrication of various composite material for various application as an electrode material for thin film supercapacitor [1, 2], photocatalyst [3], a highly selective gas sensor [4], a high-temperature solar selective absorber [5], a magnetic material [6] due to its low cost, better performance, higher theoretical capacity, stable nature, ease of availability, environmental compatibility, and different oxidation states.

Research in recent years has shown that the creation of hybrid polymer composites which comprise two or more heterogeneous nano elementary units with different properties is a promising strategy in connection with the possibility of purposeful changes in the percolation threshold, mechanical characteristics and electrical conductivity and the possibility of obtaining CM with new specified properties. However, the issue of obtaining such CMs based on various polymer matrices with the addition of carbon fillers with a modified (applied on their surface) metal (iron oxide nanoparticles), as well as the properties of such hybrid CMs, has been studied much less. The mechanical and electrophysical characteristics of hybrid CMs significantly depend on the method of CM preparation and the structural properties of each component of the CM and the distribution of components in the composite.

Addition of metal fillers, such as cobalt oxides and iron particles, to nanocarbon/polymer composites leads to changes in electrical conductivity and other important characteristics of CM [7, 8].

In the work [9] composite was made (3% $\text{Co}_3\text{O}_4$ /6%GO)- copolymer matrix of poly(aniline-copolymelamine) which exhibited the highest specific capacity due to synergy among the composite components. It is observed that as the concentration of GO was increased from 3 phr to 6 phr, the electrochemical performance of the electrode was improved. In [2] ultrathin  $\text{Co}_3\text{O}_4$  NS were grown vertically on the surface of the carbon to achieve a three dimensional composite material. The obtained composites have excellent electrochemical performance and greatly improve the electrochemical capacity. showing excellent energy storage performance. It is demonstrated that the introduction of porous carbon as substrate endows the device to maintain high energy density at high power densities.

Ternary composites of  $\text{Co}_3\text{O}_4$  nanofibers wrapped with amorphous carbon/reduced graphene oxide (rGO) can be used as chemical sensors for gases such as ammonia, methanol, ethanol, formaldehyde, benzene, acetone, and water at room temperature. The authors studied this issue [4]. In this paper, the authors studied in detail the electrical conductivity of complex ternary composites using cobalt oxide. Calculations showed that the resistances of the amorphous carbon/rGO-wrapped  $\text{Co}_3\text{O}_4$  nanofibers from S0 to S6 are about 26  $\Omega$ , 186  $\Omega$ , 4.9 k $\Omega$ , 120 k $\Omega$ , 1.5 M $\Omega$ , 9 M $\Omega$  and 24 M $\Omega$ . The nanofiber-based sensor was found to show a rapid response to ammonia at room temperature with a long-term stability of about four years, indicating significant potential for applications.

The authors of the work [10] studied the electrical

and dielectric properties of sol-gel prepared  $\text{Co}_3\text{O}_4$ /RGO nanocomposites. It was found that the conductivity of the prepared nanocomposites is thermally activated and the activation energy gradually decreases with increasing RGO loading. The observed increase of permittivity is only due to the interfacial polarization and the development of microcapacitors network.

The uniform dispersing of the  $\text{Co}_3\text{O}_4$ -GNS hybrids in TPU matrix [11] leads to a remarkable improvement of thermal stability, mechanical properties and effective reduction of fire hazards of these CMs, which were mainly attributed to the "tortuous path" effect of graphene nanosheets, catalytic char formation function of  $\text{Co}_3\text{O}_4$ -GNS hybrids and the synergism between the catalysis effect of  $\text{Co}_3\text{O}_4$  and the adsorption effect of graphene nanosheets.

In the work of the authors [12] will report on the synthesis of cobalt oxide  $\text{Co}_3\text{O}_4$  by coprecipitation. Structural analysis was confirmed by X-ray diffractometer, which showed that  $\text{Co}_3\text{O}_4$  has a cubic phase, particle size and lattice parameter of 11.87 nm and 8.082  $\text{\AA}$ . It was found that the optical band gap of  $\text{Co}_3\text{O}_4$  is 1.66 eV and 2.12 eV. The temperature dependence of dielectric permittivity and dielectric loss in the temperature range of 50-300  $^\circ\text{C}$  was investigated. The specific electrical resistance of  $\text{Co}_3\text{O}_4$  nanoparticles exhibits semiconducting behavior, which makes  $\text{Co}_3\text{O}_4$  a promising material for a supercapacitor. The value of the specific electrical resistance is  $8 \cdot 10^3$  Ohm $\cdot\text{cm}$  at 310 K, the value of the activation energy (0.16 eV) was also calculated.

The authors of another work [13] obtained  $\text{Co}_3\text{O}_4$  nanoparticles by a different method, namely by chemical deposition followed by heat treatment at different temperatures.  $\text{Co}_3\text{O}_4$  nanoparticles were obtained by chemical deposition followed by calcination at different temperatures. The results of structural studies indicate the presence of one highly crystalline  $\text{Co}_3\text{O}_4$  phase with a high surface area, a mesoporous structure, and a particle size that depends on the calcination temperature. The value of the energy band gap for optical absorption is shown as a dependence on the particle size, indicating a red shift of the absorption peaks relative to the mass  $\text{Co}_3\text{O}_4$ .

Cobalt oxide is also used to create various composites. In particular, in the work [14], nanoscale thin films of  $\text{Co}_3\text{O}_4$  on glass substrates were fabricated using the sol-gel spin-coating technology. Studies of the structure of such films have shown that all films are nanocrystallized in cubic spinel. The size of the crystallites increases with increasing annealing temperature. These modifications affect the optical properties. The morphology of the sol-gel derivative  $\text{Co}_3\text{O}_4$  shows nanocrystalline grains with some overgrown clusters, and it varies depending on the annealing temperature. The authors found that the optical band gap decreases from 2.58 eV to 2.07 eV with increasing annealing temperature between 400 $^\circ\text{C}$  and 700  $^\circ\text{C}$ . This means that the optical quality of  $\text{Co}_3\text{O}_4$  films is improved by annealing. Direct current electrical conductivity of  $\text{Co}_3\text{O}_4$  thin films varies from  $10^{-4}$  to  $10^{-2}$  (Ohm cm) $^{-1}$  with increasing annealing temperature. It is observed that annealing the  $\text{Co}_3\text{O}_4$  thin film at 700  $^\circ\text{C}$

after deposition provides a smooth and flat texture suitable for optoelectronic applications.

Therefore, the addition of cobalt oxide to various materials and the creation of composites based on it leads to the creation of materials with controlled set characteristics.

The aim of this work was to determine the effect of combining nano-sized nanocarbon fillers and  $\text{Co}_3\text{O}_4$  in different weight ratios in the epoxy matrix on the electrical conductivity and mechanical properties of the composites.

## 2. OBJECTS AND METHODS

In the manufacture of polymer composites with combined fillers, L285 epoxy resin with low viscosity ( $600\text{-}900\text{ mPa} \times \text{s}$ ) was used as a matrix, which allows for uniform distribution of various fillers in the final composite without significant deterioration of mechanical properties. Density of epoxy resin –  $1.18\text{-}1.23\text{ g/cm}^3$ .

Conductive nanocarbon particles – multi-walled carbon nanotubes (CNTs), graphite nanoplates (GNPs) and nanosized particles of cobalt oxide  $\text{Co}_3\text{O}_4$  were used as fillers.

Structural and morphological characteristics of used fillers are presented in Table 1, as well as data for carbonyl iron, which was used at fabrication of nanocarbon/Fe/L285 composites, studied in our previous works, are also given for comparison.

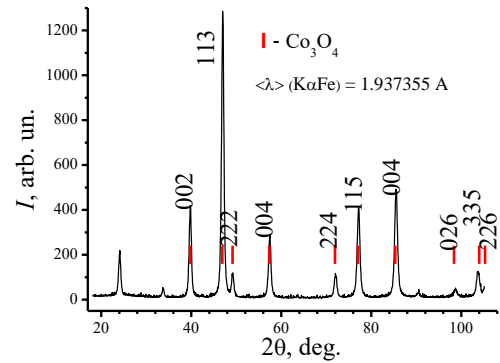
**Table 1** – Structural and morphological characteristics of fillers

Filler	Form	Particle size	AR
MWCNT	deformed cylinders	10-30 nm Length 10-30 $\mu\text{m}$	1000
GNP	plates	Lateral size - 1-10 $\mu\text{m}$ thickness - 15-45 nm	300- 500
$\text{Co}_3\text{O}_4$	spherical	< 50 nm	~ 1.2
Fe	plates	Lateral size 3-7 $\mu\text{m}$ thickness 0.6-2 $\mu\text{m}$	~ 3

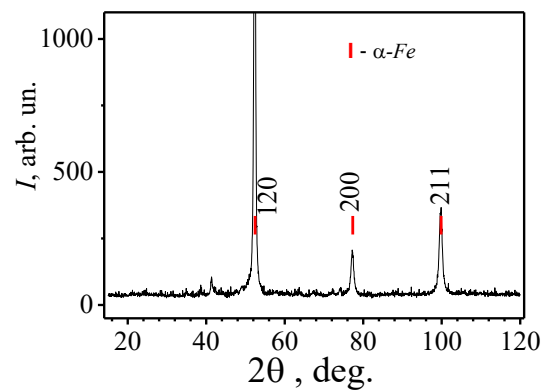
As shown by studies of the phase composition of magnetic powders by the X-ray diffraction method, cobalt oxide nanopowder consists of a pure  $\text{Co}_3\text{O}_4$  phase (Fig. 1), and carbonyl iron - of pure  $\alpha\text{-Fe}$ .

Epoxy composites with hybrid filler nanocarbon/ $\text{Co}_3\text{O}_4$  were prepared by the ultrasonic dispersing of carbon filler,  $\text{Co}_3\text{O}_4$  and epoxy mixture in acetone during the 2 hours and by pouring of the liquid mixtures into the appropriate forms for curing. Ultrasonic dispersing of composite mixture before curing leads to deagglomeration of carbon filler and provides the good dispersion of filler in epoxy matrix.

Table 2 presents data on the phase composition of manufactured samples of epoxy composites with a random distribution of combined nanocarbon/ $\text{Co}_3\text{O}_4$  fillers, as well as samples of nanocarbon/Fe/L285 for comparative analysis.



(a)



(b)

**Fig. 1** – (a) Diffraction spectra of  $\text{Co}_3\text{O}_4$  nanopowder (FeK $\alpha$  radiation) and (b) micron carbonyl iron powder (CoK $\alpha$  radiation)

**Table 2** – Phase composition of epoxy CMs with different types of combined fillers

Composition of CM	Content of carbon filler, wt. %	The content of inorganic filler wt./vol. %	Porosity of samples, P
GNP/ $\text{Co}_3\text{O}_4$ /L285	0, 2, 3, 5	30/7.8	0.12-0.15
CNT/ $\text{Co}_3\text{O}_4$ /L285	0, 2, 5	30/7.8	0.11-0.16
GNP/Fe/L285	0, 1, 2, 3, 4, 5	30/6.1	0.11-0.25
CNT/Fe/L285	1, 2, 3, 4, 5	30/6.1	0.07-0.12

The 2-probe method was used to measure the temperature dependence of electrical conductivity on direct current in the temperature range of 77-290 K, and the samples were in the form of plates with a size of  $3 \times 3 \times 7\text{ mm}^3$ .

For study the mechanical properties and changes of electrical resistance under uniaxial mechanical load, the epoxy CMs specimens were prepared as cylinders with a diameter of 3 mm and length of 7 mm. The measurement of deformation-loading diagrams and the electrical resistance of CMs under mechanical loading (compression) have been performed using an automated arrangement based on serial equipment IMASH-20-78.

## 2.1 Electrical Conductivity at Direct Current

The electrical conductivity (or electrical resistance) of polymer composites and the nature of changes in electrical properties with temperature are important characteristics that determine their prospects for various applications.

Fig. 2 shows the dependence of the electrical conductivity of the nanocarbon/inorganic filler/L285 CM on the content of nanocarbon particles, and for comparison, data for two-phase nanocarbon/epoxy resin CMs are also presented. As can be seen from the figure, the electrical conductivity of CM has a percolation character, that is, it increases sharply at a certain weight concentration  $C_{cr}$  of the nanocarbon filler [15].

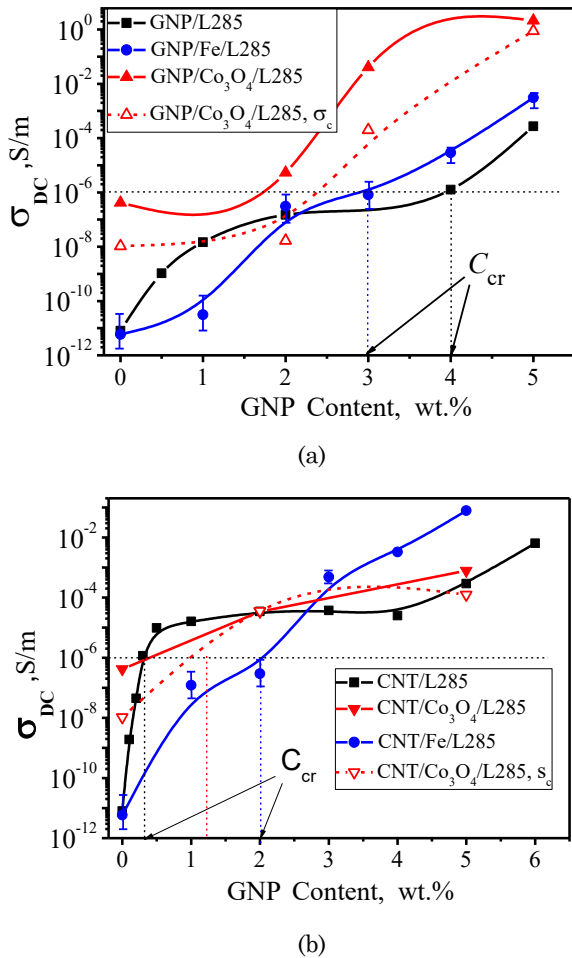


**Fig. 2** – Dependencies of direct current conductivity on the content of GNPs (a) and CNTs (b) in epoxy CMs with different types of combined fillers

The addition of inorganic fillers along with nanocarbon fillers leads to a change in the character of the percolation curves, moreover, changes in the electrical conductivity of three-phase CMs significantly depend on the size and morphology of nanocarbon particles, as well as on the nature of inorganic particles (dielectric, semiconductor, or electrical conductor). A characteristic feature of CMs with nanocarbon is significantly lower percolation thresholds for CMs with CNTs compared to GNPs, which indicates the formation of an electrically conductive network of CNTs at significantly lower contents than in GNPs/L285

CMs. This is explained by the higher aspect ratio of CNTs ( $AR \sim 1000$ ) compared to GNPs ( $AR = 100-500$ ), since the percolation threshold is directly related to the aspect ratio of filler particles:  $\sim 1.46/AR$  and  $\sim 0.53/AR$  for disc-shaped particles of GNPs and of cylindrical CNT particles, respectively [16].

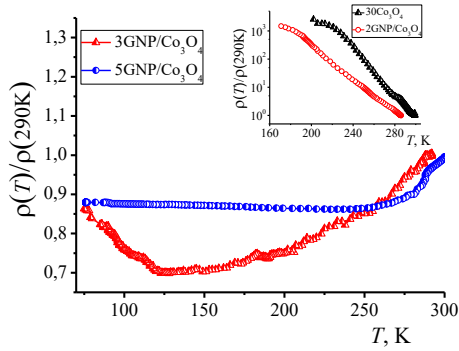
As can be seen from Fig. 2a, the electrical conductivity of two-phase CM with 30 wt. % Co<sub>3</sub>O<sub>4</sub> is quite high compared to epoxy resin ( $4.2 \cdot 10^{-7}$  S/m), which is due to the electrical nature (0.1 S/m [17]) and the nanosize of Co<sub>3</sub>O<sub>4</sub> particles, which form a large number of leading chains with a sufficiently large content of Co<sub>3</sub>O<sub>4</sub> particles (30 wt. %). On the other hand, a two-phase epoxy composite filled with 30 wt. % of lamellar micron electrically conductive Fe particles has a low electrical conductivity ( $5.9 \cdot 10^{-12}$  S/m), since at this size their concentration is small enough to overcome the percolation threshold [18]. The addition of nanocarbon filler GNP along with inorganic magnetic particles Co<sub>3</sub>O<sub>4</sub> or Fe led to a decrease in the percolation threshold and a higher electrical conductivity of CM at a GNP content higher than 3 wt. %.

At such a GNP content, electrically conductive particles of Co<sub>3</sub>O<sub>4</sub>, Fe contribute to the formation of conductive chains from GNP, connecting them together, and this effect is much greater for CM with GNP/Co<sub>3</sub>O<sub>4</sub>, since the number of Co<sub>3</sub>O<sub>4</sub> particles is much larger than Fe due to their nanosize and, accordingly, a larger number of GNP-Co<sub>3</sub>O<sub>4</sub> and Co<sub>3</sub>O<sub>4</sub>-Co<sub>3</sub>O<sub>4</sub> junctions can be formed in the conductive chains. The main role of inorganic particles in epoxy CMs with nanocarbon fillers is to improve the dispersion and homogeneity of their distribution in the epoxy matrix during the fabrication of CMs, which contributes to the effective formation of conductive chains from individual carbon nanoparticles. This effect is especially significant when electrically conductive particles (Fe, Co<sub>3</sub>O<sub>4</sub>) are used as a second filler, as well as nanosized Co<sub>3</sub>O<sub>4</sub> particles.

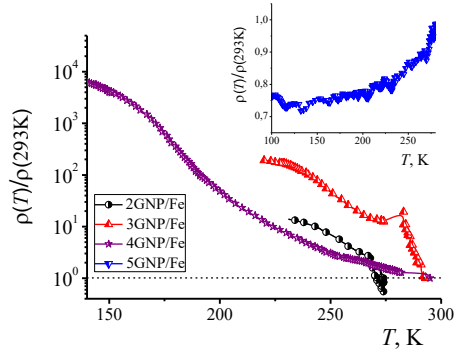
As can be seen from Fig. 2b, the adding Co<sub>3</sub>O<sub>4</sub> particles along with CNTs to the epoxy matrix, does not lead to a significant changes in the electrical conductivity at CNT content of 1-5 wt. %. This suggests the minimal influence of this type of inorganic filler on the spatial distribution of CNTs in the epoxy matrix. In the case of adding micron Fe particles together with CNTs to the epoxy matrix, an increase in the percolation threshold and an increase in electrical conductivity are observed when the CNT content is higher than 3 wt. % compared to the two-phase CNTs/L285 CM.

Figs. 3-4 show the temperature dependence of the relative electrical resistivity  $\rho(T)/\rho(290\text{ K})$  for a number of three-phase epoxy CMs.

As can be seen from the given data, the nature of the temperature dependence of the electrical resistivity is different depending on the type and content of the two-component filler in the CM. For epoxy CMs with high electrical resistivity, a significant decrease in electrical resistivity is observed upon heating from 77 to 293 K (negative temperature coefficient of resistance of TCR), for some samples this decrease is several orders of magnitude, which can be attributed to the hopping transport of electrons [19].

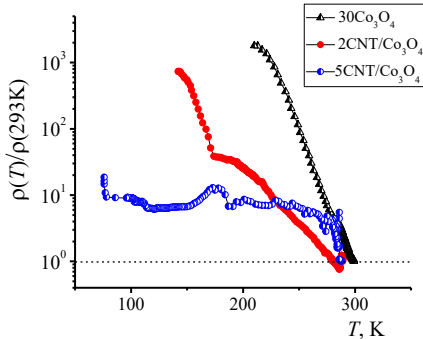


(a)

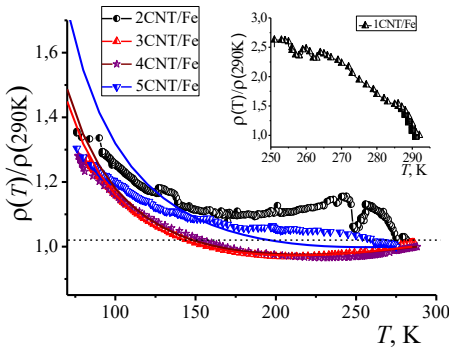


(b)

**Fig. 3** – Temperature dependence of the relative electrical resistivity for different three-phase CMs with GNP: GNP/Co<sub>3</sub>O<sub>4</sub>/L285 (a); GNP/Fe/L285 (b)



(a)



(b)

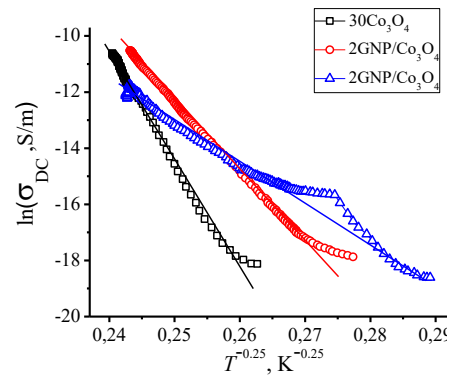
**Fig. 4** – Temperature dependence of relative electrical resistivity for different three-phase CMs with CNT: CNT/Co<sub>3</sub>O<sub>4</sub>/L285 (a); CNT/Fe/L285 (b)

If the interaction between charge carriers is neglected, the dependence of electrical conductivity on temperature can be described by the formula [19]:

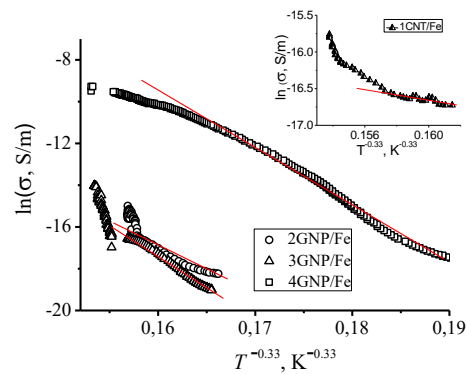
$$\sigma_{dc} = \sigma_0 \exp \left[ - \left( \frac{T_2}{T} \right)^\gamma \right], \quad (1)$$

where the  $\sigma_0$  – parameter can be regarded as the limiting value of conductivity at infinite temperature,  $T_2$  – is a characteristic temperature that determines thermally activated hopping between localized states at different energies and is considered as a measure of disorder [19], and the exponent  $\gamma$  is related to the dimensionality of the transport process by the ratio  $\gamma = 1/(1 + d)$ , where  $d = 1, 2, 3$  (dimensionality of the system). In the conventional model with a variable hopping length, the parameters  $\sigma_0$  and  $T_2$  are functions of the localization length and the density of states.

The applicability of the hopping conductivity model with variable hopping length is tested by plotting the experimental temperature dependences of electrical conductivity for three-phase CMs with low electrical conductivity in the form  $\ln(\sigma_{dc}) = f(T^{-\gamma})$ , and for CM samples with nanocarbon/Co<sub>3</sub>O<sub>4</sub> filler, good agreement between experimental and calculated data was found for  $\gamma = 1/4$  and the corresponding data are presented in Fig. 5a.



(a)



(b)

**Fig. 5** – Temperature dependences of electrical conductivity for various three-phase CMs within the framework of the jump conductivity model: a) nanocarbon/Co<sub>3</sub>O<sub>4</sub>/L285; b) nanocarbon/Fe/L285

Such a value of the parameter  $\gamma$  indicates a 3-D process of electrical transport. Table 3 presents the values of the parameter  $T_2$  that are sufficiently high ( $10^{10}$ - $10^9$ ), which indicates the low electrical conductivity of the systems and means the lack of regular arrangement of inclusions, structural disorder due to the formation of agglomerates from filler particles and the presence of dead-end branches in conductive clusters. Fig. 5b and Table 3 for comparison also show the values of parameters  $\gamma$  (0.33) for high-resistivity CM samples with nanocarbon/Fe filler, which testify to the two-dimensionality of the electrical transport process in these CMs. The difference in the nature of the conductivity for CMs with nanocarbon and various inorganic fillers indicates a different effect of nanosized  $\text{Co}_3\text{O}_4$  particles and micron Fe particles on the formation of a conductive network of filler particles in epoxy CMs.

With an increase in the content of nanocarbon fillers, especially in the case of CMs with CNTs, a significant decrease in electrical resistance of CMs, a weakening of its dependence on temperature, and the appearance of a minimum in the  $\rho(T)/\rho(293\text{K})$  dependences in the temperature range of 180-260 K are observed. Such changes in electrical resistance indicate a transition from the hopping mechanism of electrical conductivity to the tunneling mechanism, when the distance between electrically conductive particles in the chains is significantly reduced [20].

A small increase in electrical resistance above  $\sim 200$  K can be explained by an increase in the distance between nanocarbon particles due to thermal expansion of the epoxy matrix.

**Table 3** – Parameters of  $\gamma$  and  $T_2$  within the hopping conductivity model for different types of three-phase epoxy CMs

Filler	30 $\text{Co}_3\text{O}_4$	2GNP/ $\text{Co}_3\text{O}_4$	2CNT/ $\text{Co}_3\text{O}_4$	2GNP/ Fe	1CNT/ Fe
$\rho, \Omega\cdot\text{m}$	$2.4\cdot 10^6$	$1.9\cdot 10^5$	$2.9\cdot 10^4$	$3.2\cdot 10^6$	$7.0\cdot 10^6$
$\gamma$	0.25	0.25	0.25	0.33	0.33
$T_2, \text{K}$	$3.4\cdot 10^{10}$	$4.5\cdot 10^9$	$9.2\cdot 10^8$	$1.2\cdot 10^7$	$2.7\cdot 10^4$

As discussed in our previous work [21], at the first approximation, the electrical resistance of a composite consisting of a polymer matrix and a dispersed conductive component can be represented as the electrical resistance of a conductive network formed by conductive filler particles. The electrical resistance of the conductive network depends on the electrical resistance of the individual filler particles  $r_{f(ef)}$  and the contact resistance  $R_{k(ef)}$  between the filler particles in the chains.

As a rule, for polymer CMs with a content of CNT or GNP nanoparticles that does not greatly exceed the percolation threshold,  $R_{k(ef)} \gg r_{f(ef)}$  and the electrical conductivity is mainly determined by the contact resistance between the conductive particles in the chains and the number of these conductive chains. Due to the two-dimensional morphology of GNP particles, their relatively large lateral size, the contact area between them can be quite large, and the decrease in electrical resistivity during electron tunneling can be associated with an increase in the concentration of free current carriers during heating.

In the case of 1D fillers of a cylindrical shape, in particular CNTs, the area of contacts between CNTs is small enough (mainly point contacts) due to the small

size of CNTs, and the tunneling transport of current carriers also depends on the thermal motion of electrons and can be described within the framework of the fluctuation model of tunneling conductivity [22]. According to this model, the thermal motion of electrons near the tunneling barriers contributes to voltage fluctuations, which can change the probability of electron tunneling due to the reduction and narrowing of the potential barrier. Therefore, electron tunneling is highly sensitive to temperature fluctuations: the conductivity increases with increasing temperature.

Electrical transport in the investigated composites is carried out by tunneling current carriers between conductive particles or between clusters of conductive particles that are separated by thin layers (tunnel barrier width). The electrical resistivity for this case can be described within the framework of the fluctuation-induced tunneling model by the following relation [23]:

$$\rho(T) = A \exp\left(\frac{T_1}{T + T_0}\right) \exp[B \cdot \delta(T)] \cdot \delta(T), \quad (2)$$

where the parameters  $T_0$  and  $T_1$  depend on the characteristics of the tunnel barrier – the height of the barrier  $\lambda_b$ , barrier width  $\delta$  and cross-section of the barrier  $w$ :  $T_1 \sim w\lambda_b/\delta$ ,  $T_0 \sim w\lambda_b^{3/2} \delta^{3/2}$  [22];  $A$ ,  $B$  are temperature-independent parameters, the factor  $\exp(T_1/(T + T_0))$  determines the decrease in electrical resistance, the factor  $\exp[B \cdot \delta(T)] \cdot \delta(T)$  determines an increase in the resistance of the sample during heating, since the thickness of the polymer layer (the distance between electrically conductive particles) may increase during heating due to the thermal expansion of the epoxy matrix, and as a result a minimum in the dependences of  $\rho$  can be observed.

The estimation of the distance between CNT particles in the conductive chains  $\delta$  (width of the tunnel barrier) in CM CNT/Fe/L285, carried out in our previous work within the framework of the fluctuation model of tunnel conductivity [23] showed that  $\delta$  varies from 1.98 to 1.6 nm with CNT content of 3 to 5 wt. %. The value of  $\delta$  was not evaluated for the 5CNT/ $\text{Co}_3\text{O}_4$ /L285 CM due to the complexity of the observed temperature dependence of electrical resistance, which indicates the presence of both a hopping and tunneling mechanism of electrical transport in this CM.

## 2.2 Experimental Study of External Load Influence on Resistivity of Nanocarbon/ $\text{Co}_3\text{O}_4$ / Epoxy CMs

The mechanical properties and change of the electrical resistance under uniaxial compression of nanocarbon/ $\text{Co}_3\text{O}_4$ /epoxy composite were studied. Table 4 presents the elastic  $\varepsilon_{el}$  and plastic  $\varepsilon_{pl}$  deformations of specimen the effective Young's modulus and strength of the composites under compression that were derived from the experimental loading-relative deformation diagrams. As is seen from Table 4, the mechanical properties depend on the type and filler content. It was found that the addition of nanocarbon fillers along with  $\text{Co}_3\text{O}_4$  nanoparticles in epoxy matrix and increase of nanocarbon content leads to arising the plastic deformation and decrease the effective Young's

modulus and compression strength. It was found that the minimal value of Young's modulus was observed for 5CNT/30Co<sub>3</sub>O<sub>4</sub>/L285 sample and elastic deformation of this sample is highest (0.030 at 15.5 MPa) compared with other studied composites. The plastic deformation for this sample was absent, i.e. this sample is highly flexible that can be related to the deformed CNTs and entangled nature of CNTs agglomerates.

The analysis of our experimental results on electrical resistance measured under uniaxial mechanical stress has shown that the change of interparticle distance and probably filler orientation (especially in a case of GNP filler) in CMs under compression are the main reasons that lead to changes in the value of electrical resistance of studied epoxy CMs.

Table 5 shows the data on electrical resistance for the samples of nanocarbon/Co<sub>3</sub>O<sub>4</sub>/L285, which are then subjected to uniaxial mechanical stress (compression) for further resistance measuring. The stud-

ied sample have the cylinder shape and stress-load was along C-axis of cylinder and electric resistance was measured in the same direction.

**Table 4** – Effective Young's modulus and strength of epoxy composite with 30 wt. % of Co<sub>3</sub>O<sub>4</sub> and various types of nanocarbon fillers, GNPs and CNTs

Carbon filler content, wt. %	$\sigma_p$ , (1 <sup>st</sup> cycle)	$\epsilon_{pl}$	$\epsilon_{el}$	$E_{eff}$	$\sigma_c$
GNP/30Co <sub>3</sub> O <sub>4</sub> /L285					
0	16.8	~ 0	0.005	1190	75.5*
2	14.9	0.007	0.019	734	52.5*
3	16.3	0.014	0.023	708	57.5
5	14.2	0.007	0.015	950	52.4
CNT/30Co <sub>3</sub> O <sub>4</sub> /L285					
2	14.7	0.007	0.013	1100	52.9*
5	15.5	~ 0	0.030	520	81.3*

**Table 5** – Initial electrical resistivity ( $\rho$ ) of epoxy composite with 30 wt. % of Co<sub>3</sub>O<sub>4</sub> and various types of nanocarbon fillers, GNPs and CNTs

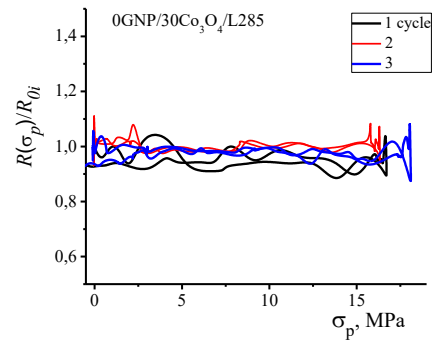
Carbon filler content, wt. %	$\rho$ , $\Omega$ m (cylinder samples)	$\sigma_p$ , (1 <sup>st</sup> cycle)	$\epsilon_{el}$	$R(\sigma_p)/R_0$ at $\sigma_p$ and after unload ( $\sigma_p = 0$ ) (1 <sup>st</sup> cycle)	$R_{fin}/R_0$ (after 3 cycles loading up to 15-16.5 MPa)	$R(\sigma_p)/R_0$ at $\sigma_c = 50$ MPa
GNP/30Co <sub>3</sub> O <sub>4</sub> /L285						
0	$9.9 \cdot 10^7$	16.8	0.012	0.88 → 0.94	1.06	0.91(0.031)
2	$5.18 \cdot 10^7$	14.9	0.026	1.16 → 1.55	1.85	0.99(0.048)
3	$4.58 \cdot 10^3$	16.3	0.037	0.07 → 1.0	0.19	0.04(0.064)
5	1.13	14.2	0.022	0.72 → 1.01	0.97	0.74(0.054)
CNT/30Co <sub>3</sub> O <sub>4</sub> /L285						
2	$2.73 \cdot 10^4$	14.7	0.020	0.39 → 0.41	0.34	0.35(0.042)
5	$7.43 \cdot 10^3$	15.5	0.030	0.17 → 0.68	1.55	0.043(0.050)

Typical dependencies of the relative electrical resistance on load compression are shown in Figs. 6-7. As seen from Fig. 6 for composite without nanocarbon filler electrical resistivity is high ( $9.9 \times 10^7 \Omega \times m$ ) and only slightly (within 10 %) changes under compression up to 17 MPa as well as for loading up to 80 MPa. The addition of 2 wt. % GNP along with 30 wt. % Co<sub>3</sub>O<sub>4</sub> into epoxy sufficiently changes the behavior of resistivity-loading diagrams: firstly electrical resistivity decreases under compression (in 2 times), i.e. passes through a minimum and then it increases and was remaining constant after unloading. The behavior of resistivity under next (2nd and 3rd) loading/unloading cycles is similar to the 1st cycle, however, the resistance value after unloading is approximately the same as at the beginning of the compression cycle. The largest decrease (by ~ 2 orders) of electrical resistivity was observed for the composite containing carbon fillers with concentrations close to the percolation threshold, namely the 3GNP/Co<sub>3</sub>O<sub>4</sub>/epoxy composite. The decrease of electrical resistivity is reversible for the 1<sup>st</sup> loading cycle, while the repeated 2<sup>nd</sup> and 3<sup>rd</sup> loading – unloading cycles lead to a large irreversible decrease of the electrical resistance and ratio of is equal 0.19 (see Table 5). The sample 5GNP/Co<sub>3</sub>O<sub>4</sub>/L285 with low initial resistivity (1.1  $\Omega \cdot m$ ) also showed the decrease of electrical resistance under compression. However, these changes are sufficiently lower compared to 3GNP/Co<sub>3</sub>O<sub>4</sub>/L285 sample, are reversible and do not exceed 30 % relative to the resistivity at the beginning

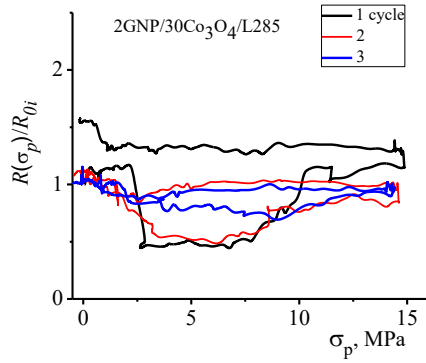
of each loading-unloading cycle. It may be concluded that at such GNP content (5 wt. %) the branched conductive 3D-network is formed and there are many direct contacts between conductive particles and contribution of tunnel transport decreases.

As seen from Fig. 7a, for 2% CNT/Co<sub>3</sub>O<sub>4</sub>/L285 the irreversible decrease of electrical resistance (in 3 times) was observed at the 1<sup>st</sup> cycle loading-unloading and at the next 2<sup>nd</sup> and 3<sup>rd</sup> cycles electrical resistance decreases reversible within the 30 % at loading up to 10 MPa.

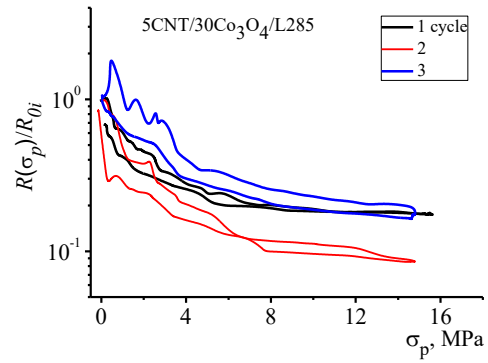
The increase of CNT content up to 5 wt. % in CNT/Co<sub>3</sub>O<sub>4</sub>/L285 composite decreases the electrical resistivity only in ~ 4 times and change (decrease) of electrical resistance at loading up to 15 MPa is much higher compared with 5 wt. % GNP/Co<sub>3</sub>O<sub>4</sub>/L285 composite (~ 1 order) that correlates with higher



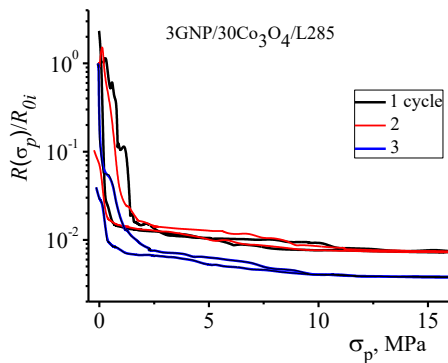
(a)



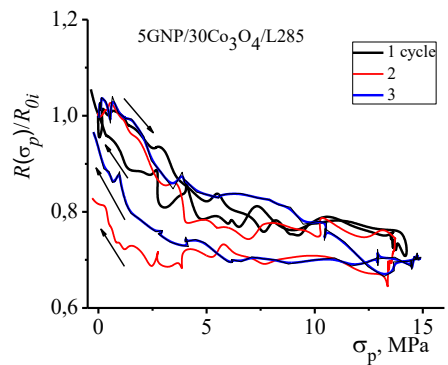
(b)



(b)

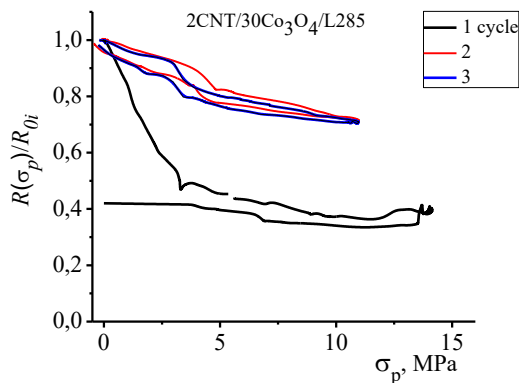


(c)



(d)

**Fig. 6** – Normalized electrical resistance of GNP/30%Co<sub>3</sub>O<sub>4</sub>/L285 CMs with various GNP content at uniaxial compression: (a) 0 wt. % GNP, (b) 2 wt. % GNP, (c) 3 wt. % GNP and (d) 5 wt. % GNP



(a)

**Fig. 7** – Normalized electrical resistance of CNT/30%Co<sub>3</sub>O<sub>4</sub>/L285 CMs with various CNT content at uniaxial compression: (a) 2 wt. % CNT, (b) 5 wt. % CNT

deformation of 5 wt. % CNT/Co<sub>3</sub>O<sub>4</sub>/L285 composite and sufficient contribution of tunnel electron transport which is highly sensitive to the change of interparticle's distance under compression (see Eq. (2)). Despite the lower percolation threshold for CMs filled with CNTs (due to their 1D morphology and high aspect ratio) compared with 2D GNP filler the tunnel contact resistance between CNTs particles is much higher due to small cross section of tunnel barrier that promotes the stronger dependence of electrical resistance versus mechanical load for the same CNT content as in a case of GNP-filled CMs.

Transformation of curves in the resistance-load cycling was caused by plastic deformations of the samples under compression, which are maximal during the first loading cycle and lead to partially irreversible changes in the microstructure of CM samples.

From the experimental results of the electrical resistance study of designed epoxy composites with different types of fillers under uniaxial compression can be concluded that changes in the CM electrical resistance essentially depend on the composite constituents and their intrinsic own electrical resistivity as well as on the direction and the value of a mechanical stress. Within the effective conductivity model [21], that takes into account the spatial distribution of carbon filler particles, their orientation in the composite, the number of particles generated conductive chains and electric contact resistance between the conductive filler particles, the electrical resistance changes in CMs under mechanical load are determined by several competing processes:

i) variation of the number of conductive paths as a consequence of the creation of new and destruction of existing during the reorientation of conductive particles (especially of carbon particles with high aspect ratio) under the influence of mechanical stress;

ii) partial destruction of electrical contacts between the conductive filler particles, as well as carbon particles themselves (the change of electrical resistance of individual carbon particles) may become significant in the presence of a large number of second filler particles (Co<sub>3</sub>O<sub>4</sub> in our case) in the composite;

iii) reduction of the electric contact resistance between the conductive filler particles by changing the contact area or the distance ( $\delta$ ) between them.



For polymer-filled composites the contact electrical resistance between filler particles is much higher than electrical resistance of individual filler particle and the change of electrical resistance of composite under uniaxial mechanical load (along C-axis) may be describes by the following relation [21]:

$$\frac{R_{CM(c)}(\theta, \varphi, \sigma_p)}{R_{CM(c)}(\theta, \varphi, 0)} \approx \frac{\cos^2 \theta(0)}{\cos^2 \theta(\sigma_p)} \cdot \frac{R_{k(c)}^*(\sigma_p)}{R_{k(c)}^*(0)}, \quad (3)$$

$$\frac{\cos^2 \theta(0)}{\cos^2 \theta(\sigma_p)} > 1, \quad \frac{R_{k(c)}^*(\sigma_p)}{R_{k(c)}^*(0)} < 1$$

where  $\theta$  is the angle between the long axis of 1D or 2D filler particle and C-axis of the cylinder samples.

Two competing processes occurred:

- increase of  $\theta$ ,  $\cos^2 \theta \downarrow$  cause increase of  $R_{CM(c)}$ ;
- decrease of  $R_{k(c)}^*$  under mechanical load  $\sigma_p$  is

caused by increase of a contact area or decrease of distance ( $\delta$ ) between conductive filler particles that cause the decrease of.

Also, it should be taken into account that partial destruction of carbon particles as a result of mechanical stress would lead to a partial increase in the average value of electric contact resistance between carbon particles.

Depending on the dominant, we will get a decrease or increase of electric resistance  $R_{CM(c)}$  during compression or even more complex non-monotonic dependence of the relative value of CM electrical on the mechanical load. The most non-monotonic dependence electrical resistance-load observed for 2%GNP/Co<sub>3</sub>O<sub>4</sub>/L285 under mechanical load (Fig. 6b) is the result of comparable competing contributions of reorientation of anisometric GNP particles (increase of the angle), possible partial destruction of conductive chains and decrease of interparticles distance (enhancing tunnel electron transport) into the change of electrical resistance. The irreversible increase of electrical resistance for this composite after repeated 3 cycles of loading-unloading ( $R_{fin}/R_0 = 1.85$ , see Table 5) testifies the irreversible reorientation and partial destruction of conductive chains. The sufficient decrease of electrical resistance under uniaxial compression for 3 %GNP/Co<sub>3</sub>O<sub>4</sub>/L285 is related to the main contribution into conductivity of tunnel electron transport and high sensitivity of tunnel contact resistance to interparticle

distance. And finally, for the sample 5 %GNP/Co<sub>3</sub>O<sub>4</sub>/L285 there are many direct contacts between conductive fillers in a large number of conductive chains, moreover the tunnel contact resistance is low due to small interparticle distance and is slightly changed under compression.

Thus, the comparative analysis of the studied three-phase CMs specimens with various nanocarbon content allows to conclude that at low nanocarbon content (~2-3 wt. %) the resistivity is high and the more complex and non-monotonous are the changes of electrical resistance under the uniaxial compression of these specimens, since the conductive network is not completely formed and highly sensitive to the deformation of the sample that affects the interparticles distances as well as spatial distribution of filler in composite. For epoxy composite with high nanocarbon filler content (~5 wt. %) the conductive network is already well-formed, number of conductive pathways is large that results in low values of electrical resistivity and lower reversible decrease of electrical resistance under uniaxial compression.

### 3. CONCLUSION

Epoxy composites with multicomponent fillers – nanocarbon (graphite nanoplatelets, carbon nanotubes)/magnetic Fe, Co<sub>3</sub>O<sub>4</sub> particles were fabricated and their structural and morphological features were investigated.

A significant increase in electrical conductivity of three-phase epoxy composites with a nanocarbon content of 3-5 wt. % compared to two-phase nanocarbon-epoxy composites was observed. The greatest increase in electrical conductivity (by 3-4 orders of magnitude) was found in composites with graphite nanoplatelets and Co<sub>3</sub>O<sub>4</sub> nanoparticles, which is related to the effective formation of a conductive network from GNP and Co<sub>3</sub>O<sub>4</sub> nanoparticles. It is shown that in CM with a nanocarbon content of up to 2 wt. %, a hopping mechanism of electrical conductivity is implemented, and an increase of the nanocarbon content up to 5 wt. % leads to the tunneling of current carriers through thin polymer layers between electrically conductive particles and clusters.

It was found, that the addition of 2-5 wt. % of graphite nanoparticles along with Co<sub>3</sub>O<sub>4</sub> nanoparticles decreases the effective Young modulus from 1190 MPa for Co<sub>3</sub>O<sub>4</sub>/epoxy to 700-950 MPa for GNP/Co<sub>3</sub>O<sub>4</sub>/epoxy CMs. The compression strength of three-phase composite also decreases compared with Co<sub>3</sub>O<sub>4</sub>/epoxy.

### REFERENCES

- S. Zallouz, B. Réty, L. Vidal, J.-M. Le Meins, C. Matei Ghimbeu, *ACS Appl. Nano Mater.* **4** No 5, 5022 (2021).
- Y. Ji, Y. Deng, F. Chen, Z. Wang, Y. Lin, Z. Guan, *Carbon* **156**, 359 (2020).
- J. Guo, Y. Zhang, Y.-C. He, J. Shan, *Polyhedron* **175**, 114215 (2020).
- Q. Feng, Y. Zeng, P. Xu, S. Lin, C. Feng, X. Li, J. Wang, *J. Mater. Chem. A* **7**, 27522 (2019).
- S. Makhlof, Z. Bakr, K. Alu, M.S. Moustafa, *Superlattice. Microst.* **64**, 107 (2013).
- K. Yin, J. Ji, Y. Shen, Y. Xiong, H. Bi, J. Sun, T. Xu, Z. Zhu, L. Sun, *J. Alloy. Compd.* **720**, 345 (2017).
- N.I. Kuskova, A.P. Malyshevskaya, S.V. Petrichenko, A.N. Yushchishchina, *Surf. Eng. Appl. Electrochem.* **47** No 5, 446 (2011).
- L. Vovchenko, O. Lozitsky, V. Oliynyk, V. Zagorodnii, T. Len, L. Matzui, Yu. Milovanov, *Appl. Nanosci.* **10** No 12, 4781 (2020).
- I. Ahmed, S. Wageh, W. Rehman, J. Iqbal, S. Mir, A. Al-Ghamdi, M. Khalid, A. Numan, *Polymers* **14**, 2685 (2022).
- A.G. Darwish, A.M. Ghoneim, M.Y. Hassaan, O.S. Shehata, G.M. Turkey, *Mater. Res. Exp.* **6**, 105039 (2019).
- K. Zhou, Z. Gui, Y. Hu, S. Jiang, G. Tang, *Composites: Part A.* **88**, 10 (2016).
- R. Bhargava, S. Khana, N. Ahmad, M. Mohsin Nizam Ansari, *2<sup>nd</sup> International Conference on Condensed Matter and Applied Physics* 030034 (ICC 2017).
- S. Makhlof, Z. Bakr, K. Alu, M.S. Moustafa, *Superlattice.*

- Microst.* **64**, 107 (2013).
14. V. Patil, P. Joshi, M. Chougule, S. Sen, *Soft Nanosci. Lett.* **2**, 1 (2012).
  15. D. Stauffer, *Introduction to Percolation Theory: Second Edition* (Taylor & Francis: 2018).
  16. L. Vovchenko, V. Vovchenko, *Materialwissenschaft Und Werkstofftechnik* **42** No 1, 70 (2011).
  17. R. Bhargava, S. Khana, N. Ahmad, *2<sup>nd</sup> International Conference on Condensed Matter and Applied Physics AIP Conf. Proc.* **1953**, 030034 (ICC 2017).
  18. Y. Mamunya, Y. Muzychenko, E. Lebedev, *Polym. Eng. Sci.* **47** No 1, 34 (2006).
  19. G. Psarras, *Compos. Part A: Appl. Sci. Manufact.* **37** No 10, 1545 (2006).
  20. N. Hu, Y. Kabure, M. Arai, *Carbon* **48** No 3, 680 (2010).
  21. L. Vovchenko, L. Matzui, Yu. Perets, I. Sagalianov, O. Yakovenko, Z. Bartul, J. Trenor, *Advances in Nanotechnology.* **21**, 1 (2018).
  22. L. Yu-Ren, Y. Kai-Fu, L. Yong-Han, *AIP Adv.* **2** No 3, 032155 (2012).
  23. T.A. Len, L.L. Vovchenko, O.V. Turkov, O.V. Lozitsky, L.Y. Matzui, *Mol. Cryst. Liq. Cryst.* **717**, 109 (2021).
  24. T.A. Len, L.Y. Matzui, I.V. Ovsiienko, Y.I. Prylutskyy, I.I. Andrievskii, I.B. Berkutov, G.E. Grechnev, *Fiz. Nizk. Temp.* **37** (9-10), 1027 (2011).

## Електричні та механічні властивості епоксидних композитів, наповнених наночастинками вуглецю та $\text{Co}_3\text{O}_4$

Т.А. Лен, Л.Л. Вовченко, Л.Ю. Мацуй, О.В. Турков, О.В. Журавков

*Київський національний університет імені Тараса Шевченка, фізичний факультет, 01601, Київ, Україна*

Проведено дослідження зразків багатокомпонентних епоксидних композитів (КМ), вивчено структуру, морфологію наповнювачів та їх розподіл в епоксидній матриці, особливості процесу модифікації електропровідного кластера та зміни міжфазної поляризації за рахунок інтеграції нановуглецевих (графітові нанопластили ВНП, вуглецеві нанотрубки УНТ) та неорганічних (Fe,  $\text{Co}_3\text{O}_4$ ) супердисперсних наповнювачів визначено вплив складу, морфології та концентрації комбінованих наповнювачів на електродинамічні характеристики композитів та механізми електротранспорту в КМ. Як показали дослідження фазового складу магнітних порошків методом рентгенівської дифракції, нанопорошок оксиду кобальту складається з чистої фази  $\text{Co}_3\text{O}_4$ , а карбонільного заліза – з чистого  $\alpha$ -Fe. Експериментальні дослідження електроопору проводилися на постійному струмі в інтервалі температур 77–293 К. Як показали дослідження, електропровідність ВМ має перколяційний характер, тобто різко зростає при певній концентрації  $C_{cr}$  або об'ємі ( $\varphi$ ) нановуглецевого наповнювача. Додавання неорганічних наповнювачів разом із нановуглецевими наповнювачами призводить до зміни характеру перколяційних кривих. Зміни електропровідності трифазних ВМ суттєво залежать від розміру та морфології нановуглецевих частинок. Додавання нановуглецевого наповнювача ВНЧ разом із неорганічними магнітними частинками  $\text{Co}_3\text{O}_4$  або Fe призводило до зниження порогу перколяції та підвищення електропровідності ВМ за вмісту ВНЧ понад 3 мас. %. При додаванні частинок  $\text{Co}_3\text{O}_4$  разом з ВНТ до епоксидної матриці відбуваються значні зміни електропровідності при вмісті УНТ 1-5 мас. % не спостерігалось. Характер температурної залежності електроопору різний в залежності від виду та вмісту двокомпонентного наповнювача в КМ. Для епоксидних КМ з високим електричним опором спостерігається значне зниження електричного опору при нагріванні від 77 до 293 К. Встановлено, що додавання 2-5 мас. % наночастинок графіту разом з наночастинками  $\text{Co}_3\text{O}_4$  знижує ефективний модуль Юнга та міцність на стиск трифазних композитів порівняно з  $\text{Co}_3\text{O}_4$ /епоксидною смолою. 5CNT/ $\text{Co}_3\text{O}_4$ /ероку СМ показав мінімальне значення модуля Юнга (520 МПа) та покращені гнучкі властивості порівняно з композитами з наповнювачем GNP/ $\text{Co}_3\text{O}_4$ . Значне зменшення електроопору (на 2 порядки) при одночасному стисненні виявлено для 3GNP/ $\text{Co}_3\text{O}_4$ /епоксидного ВМ із вмістом нанокорбону, близьким до порогу перколяції. Досить менше оборотне зниження електричного опору (не більше 30 % відносно початкового значення) спостерігалось для 5 %GNP/ $\text{Co}_3\text{O}_4$ /епоксидного композиту.

**Ключові слова:** Оксид кобальту, Композитні матеріали, Карбонільне залізо, Електропровідність, Механічні властивості.